Dalton Transactions

PAPER

Check for updates

Re–Silane complexes as frustrated lewis pairs for catalytic hydrosilylation†

Caleb A. Brown, Michael Abrahamse and Elon A. Ison [ID] *

A pathway for the catalytic hydrosilylation of carbonyl substrates with $M(C_6F_5)_3$ (M = B, Al and Ga) was calculated by DFT (B3PW91-D3) and it was shown that in the case of the Al reagent, the carbonyl substrate binds irreversibly and inhibits catalysis by generating a stable carbonyl adduct. In contrast, the reduced electrophilicity of $B(C_6F_5)_3$ disfavors the binding of the carbonyl substrate and increases the concentration of an activated silane adduct which is the species responsible for catalytic turnover. A similar mechanism was found for both cationic and neutral Re(III) species. Further, it was shown by tuning the electrophilicity of the rhenium catalysts, conditions can be found that would enable the catalytic hydrosilylation of ketone and nitrile substrates that were unreactive in previously reported systems. Thus the mechanisms proposed in this work, lay the foundation for the design of new catalytic systems.

Introduction

Catalytic hydrosilylation of carbonyls is an attractive synthetic method to protect alcohols.[1] Traditionally, hydrosilylation of carbonyls catalyzed by transition metal complexes is thought to proceed through the modified Chalk–Harrod mechanism proposed by Ojima,[2] where the first step is oxidative addition of silane to the metal center to generate a metal hydride complex. This is followed by insertion of the carbonyl substrate into the metal silyl bond resulting in a metal siloxide, which is rapidly followed by reductive elimination to yield the product.

Main group Lewis acids are also competent catalysts for hydrosilylation reactions, but are unable to undergo the oxidative addition required of the Ojima mechanism. Piers and co-workers demonstrated that the perfluorinated borane, tris (pentaflourophenyl)borane, $B(C_6F_5)_3$, was capable of catalyzing the hydrosilylation of carbonyls *via* the generation of an electrophilic silicon center.[3] The proposed mechanism proceeds *via* the activation of silane by $B(C_6F_5)_3$ to generate a frustrated Lewis pair (FLP), followed by the nucleophilic attack on silicon by the carbonyl substrate resulting in the formation of an ion pair. Hydride transfer from the ion pair releases the final product.

Oestreich and co-workers used a chiral silicon probe to demonstrate that the reaction proceeded *via* a nucleophilic attack on an electrophilic silicon center.[4] This mechanism was further supported by computational evidence from Sakata.[5]
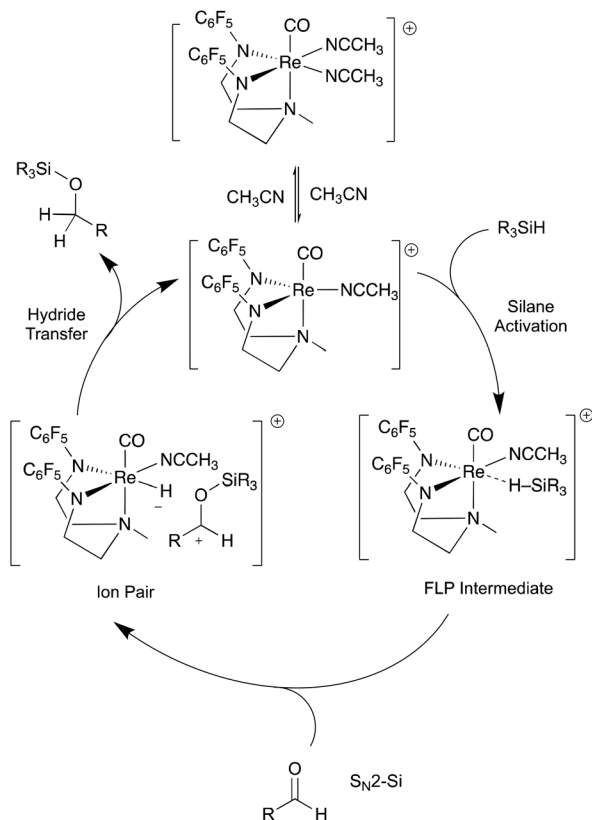
Mechanisms featuring the generation of electrophilic silicon have since been expanded to transition metal based systems for which the oxidative addition of the Si–H bond is unfavorable.[6] Toste, for example, proposed that another mechanism is viable for high valent rhenium systems which involved the [2 + 2] cycloaddition of silane across a rhenium oxo bond to generate a siloxyrhenium hydride.[7] Insertion of aldehyde into the hydride bond results in a rhenium alkoxide that undergoes a silyl group transfer group to release the final product.

Abu-Omar and coworkers described an alternative non-hydride hydrosilylation mechanism that involves an activated silane complex. Experimental work from this group has also been supported by computational studies.[8] Activation of the silane is followed by nucleophilic attack of the carbonyl substrate on the electrophilic silicon center analogous to the Piers mechanism. Brookhart also described the hydrosilylation of carbonyls with an Ir catalyst that proceeds through an activated σ-silane complex.[9] This mechanism has also been supported by mechanistic studies and DFT calculations.[10]

Recently our group reported the catalytic hydrosilylation of aldehydes by a series of cationic rhenium(III) complexes and proposed that the mechanism for this transformation is analogous to the FLP-type mechanism proposed for $B(C_6F_5)_3$ by Piers as shown in Scheme 1.[11] The catalyst was also selective for aldehydes as other carbonyl substrates (ketones, esters, amides) were not reduced under reaction conditions. In this work we provide further computational and experimental evi-

Department of Chemistry, North Carolina State University, 2620 Yarbrough Drive, Raleigh, North Carolina 27695-8204, USA. E-mail: eaison@ncsu.edu

Scheme 1 Proposed mechanism for hydrosilylation catalysed by cationic Re(III) complexes.

dence in support of this mechanism and discuss the implications for expansion of the hydrosilylation reaction to other substrates. A unified mechanism for Re catalyzed hydrosilylation based on the Piers FLP-type mechanism for $B(C_6F_5)_3$ that allows for the functionalization of weak nucleophiles has been proposed.

Results and discussion

Computational analysis of $M(C_6F_5)_3$-catalyzed (M = B, Al, Ga) hydrosilylation

In order to appropriately benchmark our study of the rhenium catalyzed hydrosilylation, we first calculated an analogous hydrosilylation reaction pathway to the one proposed by Sakata.[5] For these calculations dimethylphenylsilane and benzaldehyde were used as the representative silane and carbonyl substrate respectively. The calculated pathway is shown in Fig. 1.

As suggested by Sakata the adduct of $B(C_6F_5)_3$ and benzaldehyde, **3**, is stabilized relative to the free $B(C_6F_5)_3$ and benzaldehyde. The carbonyl substrate can dissociate to liberate the active catalyst, **1**, via **TS1** ($\Delta G^{\ddagger} = 9.5$ kcal mol^{-1}). The free Lewis acid can activate silane through **TS2** ($\Delta G^{\ddagger} = 10.0$ kcal mol^{-1}) resulting in the activated silane complex, **5**. This activated silane complex is best thought of as exhibiting FLP reactivity

which has been defined as a kinetic phenomenon whereby a Lewis acid and base act on a substrate molecule.[12] In this case the Si–H bond of the activated silane complex, is a very weak Lewis base and is a poor donor to $B(C_6F_5)_3$, resulting in a species where the electrophilicity of the Lewis acid is not completely "quenched". Indeed, the FLP reactivity of $B(C_6F_5)_3$ with silanes is known, as this species has been shown to catalyze the H/D exchange of primary silanes.[4] From Fig. 1, the carbonyl substrate nucleophilically attacks **5** at the silicon atom in the turnover-limiting step to give an ion pair, **7** ($\Delta G^{\ddagger}_{SN2–Si} = 21.8$ kcal mol^{-1}), which rapidly undergoes hydride transfer resulting in product release.

Similar mechanistic pathways for the aluminum and gallium analogs $Al(C_6F_5)_3$ and $Ga(C_6F_5)_3$ were calculated. While $Al(C_6F_5)_3$ is known to form isolable σ-silane adducts which can carry out stoichiometric hydrosilylation reactions, it is unable to carry out the catalytic hydrosilylation of carbonyl substrates.[13] Similar to the $B(C_6F_5)_3$ system, the $Al(C_6F_5)_3$-carbonyl adduct is greatly stabilized relative to the free Lewis acid and base ($\Delta G^{\circ} = -24.6$ kcal mol^{-1}). Comparison of the two pathways shows that binding of the carbonyl substrate to $Al(C_6F_5)_3$ is significantly more thermodynamically favorable than the $B(C_6F_5)_3$ system (approximately 25 kcal mol^{-1} downhill from the free Lewis acid). This is expected due to the increased electrophilicity of $Al(C_6F_5)_3$ compared to $B(C_6F_5)_3$.[14] $Ga(C_6F_5)_3$ appears to be the intermediate case for Lewis acids of this form. The free energy of the carbonyl adduct and the silane adduct are located in between the energies of $Al(C_6F_5)_3$ and $B(C_6F_5)_3$ at −11.0 and −9.2 kcal mol^{-1} respectively. The transition state energy for the nucleophilic attack of benzaldehyde on gallium is also located in between aluminum and boron systems at 14.0 kcal mol^{-1}.

Importantly, an evaluation of the equilibrium constants for the binding of benzaldehyde and dimethylphenyl silane to $B(C_6F_5)_3$, $Ga(C_6F_5)_3$, and $Al(C_6F_5)_3$ respectively, was conducted using the calculated free energies in both pathways (Table 1). While in all cases the equilibrium favors binding of the carbonyl substrate, in the $Al(C_6F_5)_3$ system, binding of benzaldehyde is approximately seven orders of magnitude more favorable than silane for $B(C_6F_5)_3$. Consequently, the ratio of the concentration of the active σ-silane complex **5** to the benzaldehyde adduct **3**, ([**5**]/[**3**]) is significantly higher for the borane catalysts (again approximately by seven orders of magnitude).

The thermodynamic stability of **3$_{Al}$** dramatically results in a significantly higher barrier for the nucleophilic attack of the carbonyl substrate on silicon (S_N2–Si, **TS3** = 33.7 kcal mol^{-1}), compared to the corresponding barriers with the boron and gallium analogs (**TS3** = 21.8 and 25.0 kcal mol^{-1} respectively). This supports the notion that the binding of the carbonyl substrate irreversibly inhibits catalysis by generating a stable carbonyl adduct **3$_{Al}$**.

In contrast, the reduced electrophilicity of $B(C_6F_5)_3$ disfavors the binding of the carbonyl substrate and increases the concentration of the activated silane adduct which is the active species responsible for catalytic turnover. Also the reaction barrier and carbonyl binding favorability trends with Lewis
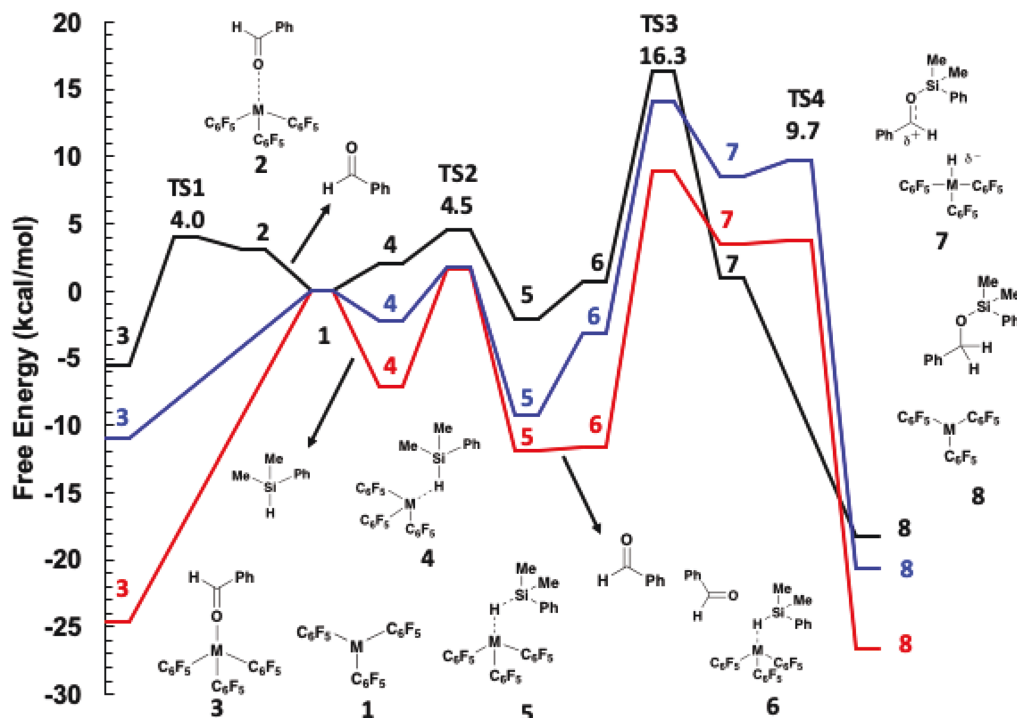
Fig. 1 Calculated pathway (B3PW91-D3) for the catalytic hydrosilylation of benzaldehyde with the catalysts $M(C_6F_5)_3$ (M = B (black), Ga, (blue), Al (red)).

Table 1 Comparison of equilibrium constants and free energies for the binding of benzaldehyde and dimethylphenylsilane to $B(C_6F_5)_3$ and $Al(C_6F_5)_3$

Entry	Comp.	K	$[5]/[3]^c$	$\Delta G^{\ddagger}$ (TS3) kcal mol^{-1}
1^a	3_B	9.30×10^{-5}	—	—
2^b	5_B	3.21×10^{1}	—	—
3^c	—	—	2.99×10^{-3}	21.8
4^a	3_{Ga}	9.16×10^{-9}	—	—
5^b	5_{Ga}	2.22×10^{2}	—	—
6^c	—	—	2.03×10^{-6}	25.0
7^a	3_{Al}	8.11×10^{-19}	—	—
8^b	5_{Al}	5.57×10^{8}	—	—
9^c	—	—	4.50×10^{-10}	33.7

^{a} Equilibrium constant for $3 \rightarrow 1$. ^{b} Equilibrium constants for $1 \rightarrow 5$. ^{c} Ratio obtained from the product of equilibrium constants for the reactions $3 \rightarrow 1$ and $1 \rightarrow 5$. $^d \Delta G^{\ddagger}$ calculated from the lowest energy structure in Fig. 1 to the highest energy structure.

acidity. Computational studies assessing the Lewis acidity of MR_3 and $M(C_6F_5)_3$ have found that the Lewis acidity follows the trend B < Ga < Al.[15] Thus from a rational design perspective being able to tune the electrophilicity of the Lewis acid appears to be critical in enabling efficient catalysis.

Analysis of Re(III)-catalyzed hydrosilylation

Computational studies. We previously reported the catalytic hydrosilylation of aldehydes with both neutral and cationic Re (III) complexes.[11] Based on the empirical rate law and a Hammett plot, we proposed that the reaction proceeded by an FLP type mechanism similar to the mechanism proposed by

Piers. In order to further understand this reaction, we carried out a detailed computational study. In this study, the electronics of the diamidoamine ancillary ligand was varied by altering the aryl substituent on the amido nitrogen (C_6F_5, and mesityl). The C_6F_5, catalyst was used successfully in the previously reported hydrosilylation of aldehydes at room temperature.[11b] In contrast, complexes incorporating the mesityl substituent were not catalytic at room temperature. The calculated pathway for a series of cationic Re(III) complexes is shown in Fig. 2.

As previously shown for the $M(C_6F_5)_3$ systems, the Re-carbonyl adducts **11**, generated by the dissociation of acetonitrile from **9** and binding of benzaldehyde, are stabilized for the DAAm ligands with mesityl and C_6F_5 substituents. Complex **9** can also dissociate acetonitrile to activate silane resulting in an activated silane complex **14** that is analogous to the activated silane complex **5** in the $M(C_6F_5)_3$ systems. Our calculations indicate that **11** is in equilibrium with **14**, so to investigate the influence of catalyst electrophilicity on this equilibrium the equilibrium constants for benzaldehyde binding and activated silane were calculated and are shown in Table 2.

Similar to the $M(C_6F_5)_3$ catalysts, benzaldehyde and silane competitively binds to the Lewis acidic transition metal center. The ratio of $[14]:[11]$ depicts the relative amounts of the active activated silane complex **14** versus the off-cycle carbonyl adduct **11**. This ratio is approximately 36 times larger for the more electrophilic C_6F_5 substituted complex compared to the more electron rich and sterically hindered mesityl substituted ligand. In addition, the energy of the highest transition state on the potential energy surface corresponds to S_N2–Si attack of the carbonyl substrate on the silane. This transition state is
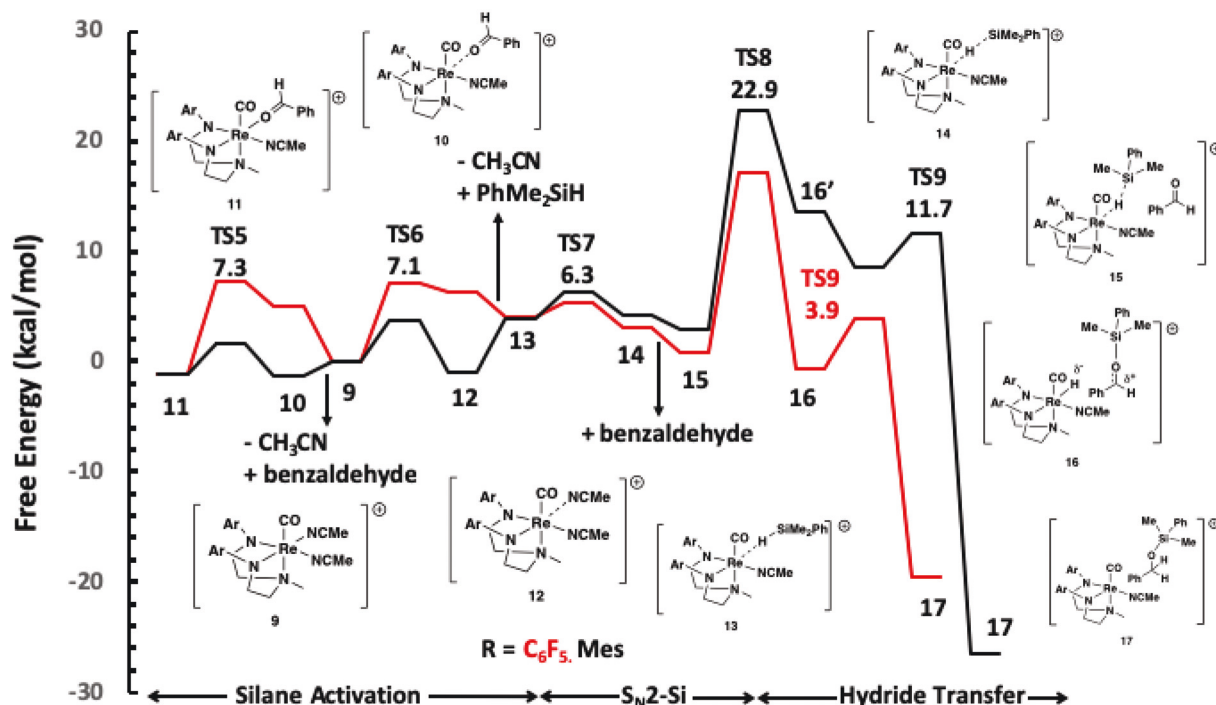
Fig. 2 Calculated pathway (B3PW91–D3) for the catalytic hydrosilylation of benzaldehyde with the catalysts [DAAmRe(CO)(NCCH$_3$)$_2$]$^+$ (DAAm = DAAm = N,N-bis(2-arylaminoethyl)methylamine; aryl = C$_6$F$_5$, Mes).

Table 2 Comparison of equilibrium constants and free energies for the binding of benzaldehyde and dimethylphenylsilane to DAAmRe(CO)(NCCH$_3$)$_2$ + (DAAm = DAAm = N,N-bis(2-arylaminoethyl)methylamine; aryl = C$_6$F$_5$, Mes, Ph)

Entry	Comp	K_{eq}	[14]/[11]^c	$\Delta G^{\ddagger\,d}$ (kcal mol^{-1})
1^a	**11$_{C6F5}$**	5.01 × 10^{-1}	—	18.3
2^b	**14$_{C6F5}$**	4.87 × 10^{-2}	—	—
3^c	—	—	2.43 × 10^{-2}	—
4^a	**11$_{Mes}$**	4.30 × 10^{-1}	—	23.9
5^b	**14$_{Mes}$**	1.56 × 10^{-3}	—	—
6^c	—	—	6.70 × 10^{-4}	—
7^a	**11$_{acet}$**	3.95 × 10^{-8}	—	28.7
8^b	**14$_{acet}$**	4.87 × 10^{-2}	—	—
9^c	—	—	1.92 × 10^{-9}	—

^{a} Equilibrium constant for **11** → **9**. ^{b} Equilibrium constant for **9** → **14**. ^{c} Ratio obtained from the product of equilibrium constants for the reactions **11** → **9** and **9** → **14**. ^{d} $\Delta G^{\ddagger}$ calculated from the lowest energy structure in Fig. 2 to the highest energy structure.

5.6 kcal mol^{-1} lower in energy for the C$_6$F$_5$ complex compared to the mesityl substituted analog.

Experimentally reactions catalyzed with the C$_6$F$_5$ substituted catalysts go to completion in a few hours at room temperature at catalyst loadings as low as 0.1 mol%. In contrast, catalysis with the mesityl substituted ligands require heating to 80 °C overnight at much higher catalyst loadings (5 mol%). These data appear to be consistent with the computational results and suggests that the electronics of the substituent on the diamido ligand has a significant impact on controlling the electrophilicity of the transition metal centre.

Chemoselectivity and implications for expansion of the substrate scope. Our calculations indicate that $\Delta G^{\ddagger}$ for hydrosilylation was dependent on both the amount of stabilization gained by substrate binding and the barrier for S$_N$2-Si. We used this result to further understand the selective reduction of aldehydes in the presence of ketones, which should be more nucleophilic and undergo S$_N$2–Si more rapidly. Pathways for the hydrosilylation of benzaldehyde and acetophenone catalyzed by [DAAmRe(CO)(NCCH$_3$)$_2$]$^+$ (DAAm = N,N-bis(2-arylaminoethyl)methylamine; aryl = C$_6$F$_5$) are compared (see ESI†). Comparisons of the equilibrium constants for the binding of acetophenone and silane are shown in Table 2 and clearly demonstrate that the origin for the selectivity is primarily due to the position of the equilibrium of the carbonyl adduct **11** and its relative concentration compared to **14**. Strong binding of acetophenone results in a ratio of [**14**]/[**11**] that is approximately seven orders of magnitude smaller than the corresponding reaction with benzaldehyde. Further, because the acetophenone adduct is significantly stabilized relative to the starting complex **9** ($\Delta G^{\circ} = -10.1$ kcal mol^{-1}) the overall activation energy for the S$_N$2–Si step for acetophenone (28.7 kcal mol^{-1}) is significantly larger than the benzaldehyde reaction (18.3 kcal mol^{-1}). The enhanced stabilization of the rhenium-acetophenone adduct **11$_{acet}$**, results in inhibition of reactivity for this substrate at room temperature. This is reminiscent of the reactivity of Al(C$_6$F$_5$)$_3$ with carbonyl substrates.

Ketone hydrosilylation. Catalysis of ketones can be achieved with the neutral Re(III) catalysts [DAAmRe(CO)(X)] (DAAm = N,N-bis(2-arylaminoethyl)methylamine; aryl = C$_6$F$_5$, X = OAc,
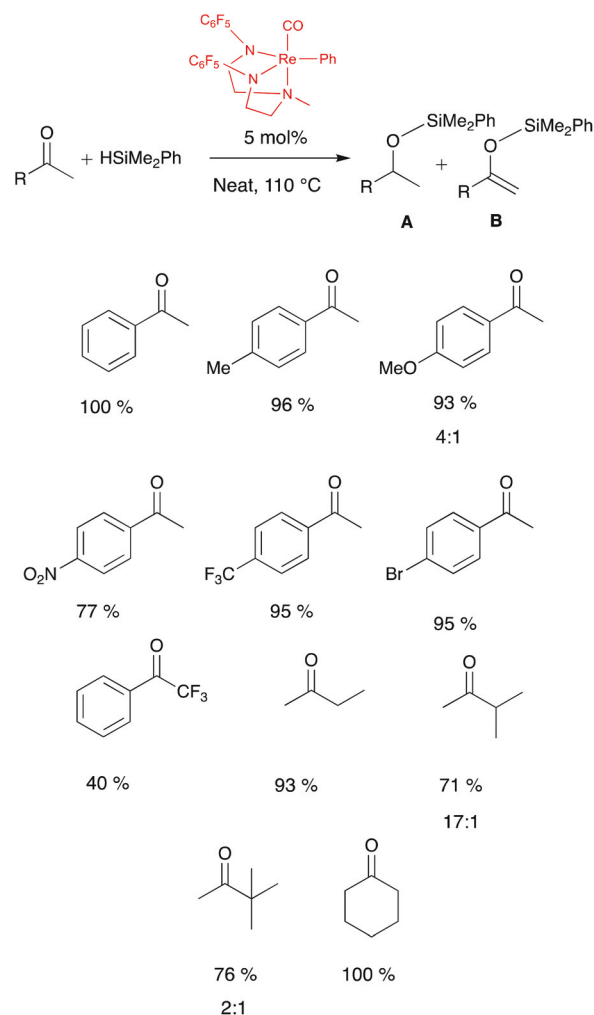
Ph) and the cationic catalyst $[DAAmRe(CO)(NCCH_3)_2]^+$ (DAAm = N,N-bis(2-arylaminoethyl)methylamine; aryl = C_6F_5), upon heating to 110 °C and performing the reaction with significantly higher catalyst loadings (5 mol% compared to 0.1 mol% for aldehydes). Neutral Re(III) complexes were previously shown to be efficient for the catalytic hydrosilylation of aldehydes.[11a] We show below that catalytic reactions with the neutral catalyst proceed with a similar pathway to the cationic catalysts described above.

Notably for the catalytic hydrosilylation of ketones, more forcing conditions are needed because the nucleophilic carbonyl substrate binds competitively with the electrophilic rhenium center. At higher temperatures, the ratio of [**14**]/[**11**] is increased to allow for efficient hydrosilylation of a variety of ketones. In addition to the expected silyl ether, **A**, the silyl enol ether **B**, was also observed when the neutral catalyst, [DAAmRe(CO)(OAc)] (DAAm = N,N-bis(2-arylaminoethyl)methylamine; aryl = C_6F_5) and the cationic catalyst $[DAAmRe(CO)(NCCH_3)_2]^+$ (DAAm = N,N-bis(2-arylaminoethyl)methylamine; aryl = C_6F_5) were used. The scope of ketone hydrosilylation was explored with the neutral catalyst [DAAmRe(CO)(Ph)] (DAAm = N,N-bis(2-arylaminoethyl)methylamine; aryl = C_6F_5) to limit the formation of **B** (Scheme 2).
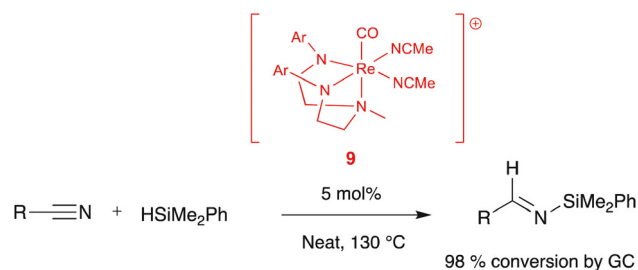
Excellent yields were observed for most substrates with the exception of the electron poor *para*-nitroacetophenone and 2,2,2-trifluoroacetophenone, which showed significantly reduced activity. The formation of **B** was also observed for the hydrosilylation of *para*-methoxyacetophenone. This product was also observed as the sterics on aliphatic substrates were increased. This suggests that both steric and electronic factors play a role in favoring formation of the silyl ether over the silyl enol ether.

Nitrile hydrosilylation. With this encouraging result we also calculated the free energy barrier for the hydrosilylation of benzonitrile. Benzonitrile binding to **9** was also found to be exergonic ($\Delta G^\circ = -7.5$ kcal mol^{-1}). The barrier for the nucleophilic attack of benzonitrile on silicon **TS**$_{SN2-Si}$ ($\Delta G^\ddagger = 16.6$ kcal mol^{-1}) and the overall hydrosilylation barrier for nitrile reduction was found to be 24.1 kcal mol^{-1}. These data suggest that nitrile hydrosilylation should be accessible with heating. As shown in Scheme 3, hydrosilylation of benzonitrile to the silyl imine was achieved with catalyst **9** (5 mol%) at 130 °C.

Mechanism for catalytic hydrosilylation with neutral Re(III) complexes. We previously proposed a pathway for the catalytic hydrosilylation of benzaldehydes with the neutral Re(III) complex, [DAAmRe(CO)(OAc)] (DAAm = N,N-bis(2-arylaminoethyl)methylamine; aryl = C_6F_5) that involved the initial generation of a rhenium hydride after silane abstraction by the metal center (Scheme 4).[11a] This was supported by the isolation of a dirhenium complex from the stoichiometric reaction with silane. This dirhenium complex was not catalytically active but was isolated in the absence of the carbonyl substrate which suggests that this species resulted from the formation of a Re–H followed by reductive elimination. The present data have allowed us to revisit this mechanism to include the presence of an activated silane complex as an FLP intermediate (Scheme 4).
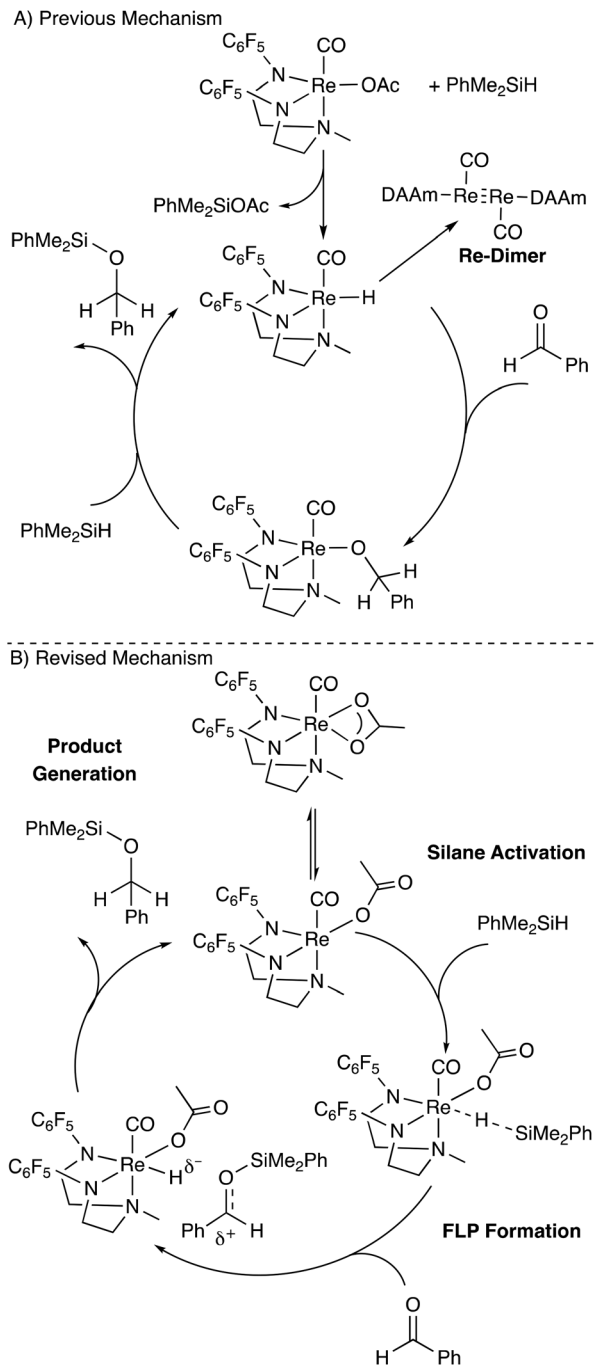

Scheme 2 Substrate scope of ketone hydrosilylation. Catalysis performed with [DAAmRe(CO)(X)] (DAAm = N,N-bis(2-arylaminoethyl) methylamine; aryl = C_6F_5, X = Ph). Spectroscopic yields determined by integration of product signal by ^{1}H NMR spectroscopy of the methine proton (silyl ether) or the alkene proton (silyl enol ether) against the aromatic signal of a mesitlyene internal standard (0.135 mmol).

Scheme 3 . Hydrosilylation of benzonitrile. Catalysis performed with [DAAmRe(CO)(OAc)] (DAAm = N,N-bis(2-arylaminoethyl)methylamine; aryl = C_6F_5). Yields determined by GC.

The pathway was also explored computationally (see ESI†). Nucleophilic attack of benzaldehyde on an activated silane complex, **23**, occurs to generate the ion pair. The ion pair

Scheme 4 Previous and revised proposed mechanisms for catalytic hydrosilylation reactions with neutral Re(III) complexes.

The kinetics for the catalytic reaction were also obtained for this system. The hydrosilylation of equimolar solutions of benzaldehyde and dimethylphenylsilane resulted in linear fits to (1/[PhCHO]). In contrast, fits to ln[PhCHO] were non-linear (see ESI†). In addition, the dependence on the rhenium catalyst was also linear (see ESI†).

These data lead to the empirical rate law:

$$\frac{d[\text{PhCHO}]}{dt} = k_{\text{abs}}[\text{Benzaldehyde}][\text{Silance}] \qquad (1)$$

$$k_{\text{abs}} = k[\text{Re}] \qquad (2)$$

which is consistent with the computational data. In addition, we previously reported a KIE of 1.4 for catalytic reactions employing PhMe$_2$SiH and PhMe$_2$SiD.[11a] This KIE is consistent with the activation of (but not cleavage) of silane prior to the turnover limiting step as predicted in the calculated mechanism. Thus, this revised mechanistic picture offers a unified understanding of hydrosilylation catalyzed by these Re(III) complexes that involves an activated silane complex that exhibits FLP reactivity.[16]

Analysis and comparison of metal–silane FLP structures. In order to gain a better understanding of the exact nature of the proposed activated silane frustrated Lewis pairs we conducted an energy decomposition analysis (EDA) on the optimized FLP structures using the AOMix program by Gorelsky.[26] To implement this calculation the complexes are divided into chemically relevant fragments, (Chart 1).

The interaction energy (E_{int}) between these fragments is then calculated and decomposed into the orbital overlap contribution (E_{Orb}) and an electrostatic contribution (E_{Steric}). It is important to note, E_{Steric} contains contributions from both the Pauli exchange repulsion energy (E_{EX}), as well as from classical electrostatic interaction energies (E_{ES}). The results of the EDA calculations are shown in Table 3.

In an FLP, strong covalent bonding between the Lewis acid/base is minimized due to steric or electronic constraints. Therefore the forces responsible for holding the molecules together becomes predominantly noncovalent interactions. The relative contributions of noncovalent/covalent interactions can be obtained by inspecting the absolute value of the ratio of the orbital interaction energy to the steric energy ($|E_{\text{orb}}/E_{\text{steric}}|$) with values close to 1 suggesting equal contributions of covalent and non-covalent interactions.

undergoes rapid hydride transfer to release the product. As in the mechanisms for the M(C$_6$F$_5$)$_3$ and cationic Re(III) systems, benzaldehyde competes with silane for binding to the metal center to produce the benzaldehyde adduct **21**. The ratio of [**23**]/[**21**] was calculated to be 4.51×10^{-3} which is comparable to the corresponding ratio with the B(C$_6$F$_5$)$_3$ catalyst (2.99×10^{-3}) but is lower than the cationic rhenium(III) catalyst [DAAmRe(CO)(NCCH$_3$)$_2$]$^+$ (DAAm = N,N-bis(2-arylaminoethyl)methylamine; aryl = C$_6$F$_5$) (2.43×10^{-2}).
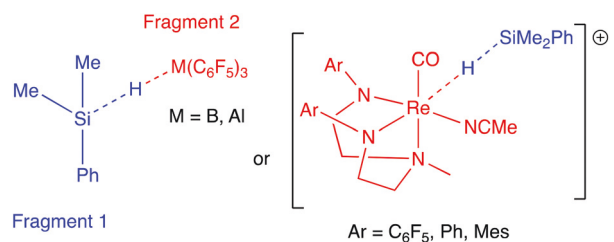

Chart 1 Fragments for EDA analysis.

Table 3 Energy decomposition analysis of *in situ* generated frustrated lewis pairs

Entry	Comp.	E_{orb} (kcal mol^{-1})	E_{steric} (kcal mol^{-1})	$|E_{orb}/E_{steric}|$
1	**5$_B$**	−53	22	2.3
2	**5$_{Ga}$**	−42	4.7	8.9
3	**5$_{Al}$**	−35	3	12.9
4	**14$_{C6F5}$**	−13	−11	1.1
5	**14$_{Ph}$**	−71.6	26.6	2.4
6	**14$_{Mes}$**	−31	−4	7.9
7	**23**	−23	−3	8.5
8	**27**	−18	−14	1.3
9	**28**	−10	−7	1.5

By using reference points of known adducts and FLP's a more nuanced picture can be described, with high values associated with classical adducts, while lower ratios are associated with FLP's. This is illustrated by the $|E_{orb}/E_{steric}|$ ratio for MesReO–B(C$_6$F$_5$)$_3$, **27**, and lutidine–B(C$_6$F$_5$)$_3$, **28**, both of which are known to exhibit FLP reactivity.[17] The ratios for these complexes are 1.3 and 1.5 respectively. Intermediate **13$_{C6F5}$**, which is very active for hydrosilylation has a the $|E_{orb}/E_{steric}|$ ratio 1.1. This is consistent with its assignment as an FLP. Intermediates **14$_{Ph}$** and **14$_{Mes}$** have less FLP character with absolute ratios of 2.4 and 7.9 respectively, which is consistent with their diminished reactivity. The neutral Re(III) catalyst **23** has an absolute ratio of 8.5, which is again consistent with the requirement for harsher conditions (temperature and catalyst loading) required to achieve high conversion when **18** is used as a catalyst. Finally, **5$_{Al}$** which was shown to be inactive for the catalytic hydrosilylation of carbonyl substrates has an $|E_{orb}/E_{steric}|$ ratio of 12.9.

A trend is also clear when the length of the Si–H bonds in the activated complexes are compared. Intermediate **14$_{C6F5}$** has the most elongated Si–H bond (1.591 Å) followed by **5$_B$** with an Si–H bond length of 1.563 Å, and **23** with an Si–H bond length of 1.542 Å. These are all elongated from the unactivated Si–H bond length of 1.494 Å, but are significantly shorter than the 1.703 Å average of η^2 Si–H bonds of transition metal silane complexes contained in the CCSD, and shorter still than the average (2.500 Å) Si–H bonds of known silyl metal hydrides. Importantly, the trend in Si–H bond length mirrors the trend in $|E_{orb}/E_{steric}|$, where lower ratios correspond to increased FLP character, increased silane activation, and increased catalytic activity in carbonyl hydrosilylation.

Conclusions

The off-cycle equilibrium binding of carbonyl substrates is an important factor in determining the activity of Lewis acids in hydrosilylation catalysis, and is consistent with the observation that strong Lewis acids such as Al(C$_6$F$_5$)$_3$ are unable to catalyze the hydrosilylation of carbonyl substrates. The mechanism for Re catalyzed hydrosilylation is best described by the FLP mechanism first proposed by Piers for the B(C$_6$F$_5$)$_3$ catalysts with an activated Re(III) silane intermediate that exhibits FLP reactivity. An energy decomposition analysis (EDA) study suggest that the frustrated Lewis pair reactivity arises from a change in the ratio of orbital and steric energy contributions to the interaction energy between the Lewis acid and base. This allows frustrated Lewis pairs and adducts to be described by a spectrum of reactivity. Understanding the nature of covalent and non-covalent interactions within this spectrum has important implications for the rational design of new catalysts.

It was also shown that controlling the Lewis acidity of the metal component is critical for the selectivity of catalytic hydrosilylation. This strategy has allowed for the reduction of ketones and nitriles which were unreactive under previously reported conditions. The FLP reactivity described is most likely quite general for rhenium complexes and the mechanisms proposed here lay the foundation for the design of new catalytic systems.

Experimental section

General considerations

Complexes **9$_{C6F5}$**, **9$_{Mes}$**, and **18** were prepared as reported in the literature.[11] All reactions were conducted under nitrogen in a glovebox or using standard Schlenk line techniques unless otherwise noted. All other reagents were purchased from commercial sources and used as received. ^{1}H, ^{13}C, and ^{19}F NMR spectra were obtained on a Varian Mercury 400 MHz, a Varian Mercury 300 MHz, or a Brüker 500 or 700 MHz spectrometer at room temperature. Chemical shifts are listed in parts per million (ppm) and referenced to the residual protons or carbons of the deuterated solvents respectively. Elemental analyses were performed by Atlantic Microlabs, Inc. X-ray crystallography was performed at the X-ray Structural Facility of North Carolina State University.

General procedure for kinetic profiles

The rhenium catalyst was dissolved in 0.25 mL benzaldehyde (2.46 mmol) and 0.38 mL dimethylphenyl silane (2.46 mmol) was added to the solution. Mesitylene 0.34 mL (2.46 mmol), was then added as an internal standard. The reaction was then divided into 0.1 mL aliquots and placed in screwcap NMR tubes. The reaction was then heated at 80 °C for the appropriate time. Deuterated chloroform was then added to reaction mixture. The product and benzaldehyde concentrations were determined using ^{1}H NMR spectroscopy to compare the integral of the product peak to the signal for the aromatic protons of the internal standard.

General procedure for ketone hydrosilylation reactions

The rhenium catalyst was added to a screwcap NMR tube and dissolved in ketone (0.135 mmol). Dimethylphenyl silane (0.406 mmol) was then added to the solution. The reaction was then heated at 110 °C for 24 hours. Deuterated chloroform and an internal standard (mesitylene, 0.135 mmol) was then added to reaction mixture. The %conversion was determined

using ^{1}H NMR spectroscopy to compare the integral of the product peak to the signal for the aromatic protons of the internal standard.

Computational methods

Theoretical calculations have been carried out using the Gaussian 09[18] implementation of B3PW91[19] density functional theory with the D3 version of Grimme's empirical dispersion correction.[20] All geometry optimizations were carried out in the gas phase using tight convergence criteria ("opt = tight") and pruned ultrafine grids ("Int = ultrafine"). The basis set for rhenium was the small-core (311111,22111,411) → [6s5p3d] Stuttgart–Dresden basis set and relativistic effective core potential (RECP) combination (SDD) with an additional f polarization function.[21] The 6-31G(d,p) basis set[22] was used for all other atoms. All structures were fully optimized. Analytical frequency calculations were performed on all structures to ensure either a zeroth-order saddle point, (a local minimum), or a first-order saddle point (transition state: TS) was achieved. The minima associated with each transition state were determined by animation of the imaginary frequency.

Energetics were calculated on the gas phase optimized structures as described above with the 6-311++G(d,p)[23] basis set for C, H, N, O and F atoms and the SDD[21a–m,24] basis set with an added f polarization function[21n] on Re. Reported energies utilized analytical frequencies and the zero point corrections from the gas phase optimized geometries and **did not include solvent corrections**.[25] Mulliken population analysis (MPA) and energy decomposition analysis (EDA) were performed using AOMix 6.90.[26]

Conflicts of interest

There are no conflicts to declare.

Acknowledgements

Notes and references

1 (*a*) B. Marciniec, *Comprehensive handbook on hydrosilylation*, Pergamon Press, Oxford, New York, 1992; (*b*) I. Ojima, in *The Chemistry of Organic Silicon Compounds*, ed. S. Patai and Z. Rappoport, John Wiley & Sons, New York, 1989, p. 1479.

2 (*a*) M. N. I. Ojima and Y. Nagai, *Bull. Chem. Soc. Jpn.*, 1972, **45**, 3722; (*b*) I. Ojima, M. Nihonyanagi and Y. Nagai, *J. Chem. Soc., Chem. Commun.*, 1972, 938a; (*c*) O. Iwao and N. Yoichiro, *Chem. Lett.*, 1974, **3**, 223–228; (*d*) I. Ojima, T. Kogure, M. Kumagai, S. Horiuchi and T. Sato, *J. Organomet. Chem.*, 1976, **122**, 83–97; (*e*) N. Schneider, M. Finger, C. Haferkemper, S. Bellemin-Laponnaz, P. Hofmann and L. H. Gade, *Chem. – Eur. J.*, 2009, **15**, 11515–11529.

3 (*a*) D. J. Parks and W. E. Piers, *J. Am. Chem. Soc.*, 1996, **118**, 9440–9441; (*b*) D. J. Parks, J. M. Blackwell and W. E. Piers, *J. Org. Chem.*, 2000, **65**, 3090–3098; (*c*) A. Y. Houghton, J. Hurmalainen, A. Mansikkamäki, W. E. Piers and H. M. Tuononen, *Nat. Chem.*, 2014, **6**, 983–988.

4 S. Rendler and M. Oestreich, *Angew. Chem., Int. Ed.*, 2008, **47**, 5997–6000.

5 K. Sakata and H. Fujimoto, *J. Org. Chem.*, 2013, **78**, 12505–12512.

6 M. Iglesias, F. J. Fernández-Alvarez and L. A. Oro, *ChemCatChem*, 2014, **6**, 2486–2489.

7 K. A. Nolin, J. R. Krumper, M. D. Pluth, R. G. Bergman and F. D. Toste, *J. Am. Chem. Soc.*, 2007, **129**, 14684–14696.

8 (*a*) G. Du, P. E. Fanwick and M. M. Abu-Omar, *J. Am. Chem. Soc.*, 2007, **129**, 5180–5187; (*b*) G. Du and M. M. Abu-Omar, *Organometallics*, 2006, **25**, 4920–4923; (*c*) P. Gu, W. Wang, Y. Wang and H. Wei, *Organometallics*, 2013, **32**, 47–51.

9 S. Park and M. Brookhart, *Organometallics*, 2010, **29**, 6057–6064.

10 (*a*) T. T. Metsänen, P. Hrobárik, H. F. T. Klare, M. Kaupp and M. Oestreich, *J. Am. Chem. Soc.*, 2014, **136**, 6912–6915; (*b*) T. Robert and M. Oestreich, *Angew. Chem., Int. Ed.*, 2013, **52**, 5216–5218.

11 (*a*) J. L. Smeltz, P. D. Boyle and E. A. Ison, *Organometallics*, 2012, **31**, 5994–5997; (*b*) D. E. Pérez, J. L. Smeltz, R. D. Sommer, P. D. Boyle and E. A. Ison, *Dalton Trans.*, 2017, **46**, 4609–4616.

12 F.-G. Fontaine and D. W. Stephan, *Philos. Trans. R. Soc., A*, 2017, **375**, 20170004.

13 J. Chen and E. Y. X. Chen, *Angew. Chem., Int. Ed.*, 2015, **54**, 6842–6846.

14 E. Y.-X. Chen, in *Encyclopedia of Reagents for Organic Synthesis*, 2012, DOI: 10.1002/047084289X.rn01382.

15 (*a*) H. Böhrer, N. Trapp, D. Himmel, M. Schleep and I. Krossing, *Dalton Trans.*, 2015, **44**, 7489–7499; (*b*) A. Y. Timoshkin and G. Frenking, *Organometallics*, 2008, **27**, 371–380.

16 For a recent example with a ruthenium sytem, see: Y.-F. Yang, L. W. Chung, X. Zhang, K. N. Houk and Y.-D. Wu, *J. Org. Chem.*, 2014, **79**, 8856–8864.

17 (*a*) N. S. Lambic, R. D. Sommer and E. A. Ison, *J. Am. Chem. Soc.*, 2016, **138**, 4832–4842; (*b*) S. J. Geier and D. W. Stephan, *J. Am. Chem. Soc.*, 2009, **131**, 3476–3477; (*c*) N. S. Lambic, R. D. Sommer and E. A. Ison, *ACS Catal.*, 2017, **7**, 1170–1180.

18 M. J. Frisch, G. W. Trucks, H. B. Schlegel, G. E. Scuseria, M. A. Robb, J. R. Cheeseman, G. Scalmani, V. Barone, G. A. Petersson, H. Nakatsuji, X. Li, M. Caricato, A. Marenich, J. Bloino, B. G. Janesko, R. Gomperts, B. Mennucci, H. P. Hratchian, J. V. Ortiz, A. F. Izmaylov,

J. L. Sonnenberg, D. Williams-Young, F. Ding, F. Lipparini, F. Egidi, J. Goings, B. Peng, A. Petrone, T. Henderson, D. Ranasinghe, V. G. Zakrzewski, J. Gao, N. Rega, G. Zheng, W. Liang, M. Hada, M. Ehara, K. Toyota, R. Fukuda, J. Hasegawa, M. Ishida, T. Nakajima, Y. Honda, O. Kitao, H. Nakai, T. Vreven, K. Throssell, J. A. Montgomery Jr., J. E. Peralta, F. Ogliaro, M. Bearpark, J. J. Heyd, E. Brothers, K. N. Kudin, V. N. Staroverov, T. Keith, R. Kobayashi, J. Normand, K. Raghavachari, A. Rendell, J. C. Burant, S. S. Iyengar, J. Tomasi, M. Cossi, J. M. Millam, M. Klene, C. Adamo, R. Cammi, J. W. Ochterski, R. L. Martin, K. Morokuma, O. Farkas, J. B. Foresman and D. J. Fox, *Gaussian 09, Revision D.01*, Gaussian, Inc., Wallingford CT, 2016.

19 (*a*) A. D. Becke, *Phys. Rev. A*, 1988, **38**, 3098; (*b*) A. D. Becke, *J. Chem. Phys.*, 1993, **98**, 5648–5652.

20 S. Grimme, J. Antony, S. Ehrlich and H. Krieg, *J. Chem. Phys.*, 2010, **132**, 154104.

21 (*a*) X. Cao and M. Dolg, *J. Chem. Phys.*, 2001, **115**, 7348–7355; (*b*) X. Cao and M. Dolg, *J. Mol. Struct.: THEOCHEM*, 2002, **581**, 139–147; (*c*) T. Leininger, A. Nicklass, H. Stoll, M. Dolg and P. Schwerdtfeger, *J. Chem. Phys.*, 1996, **105**, 1052–1059; (*d*) A. Nicklass, M. Dolg, H. Stoll and H. Preuss, *J. Chem. Phys.*, 1995, **102**, 8942–8952; (*e*) W. Küchle, M. Dolg, H. Stoll and H. Preuss, *J. Chem. Phys.*, 1994, **100**, 7535–7542; (*f*) M. Dolg, H. Stoll, H. Preuss and R. M. Pitzer, *J. Phys. Chem.*, 1993, **97**, 5852–5859; (*g*) U. Häussermann, M. Dolg, H. Stoll, H. Preuss, P. Schwerdtfeger and R. M. Pitzer, *Mol. Phys.*, 1993, **78**, 1211–1224; (*h*) P. Fuentealba, L. v. Szentpaly, H. Preuss and H. Stoll, *J. Phys. B: At. Mol. Phys.*, 1985, **18**, 1287–1296; (*i*) H. Stoll, P. Fuentealba, P. Schwerdtfeger, J. Flad, L. v. Szentpály and H. Preuss, *J. Chem. Phys.*, 1984, **81**, 2732–2736; (*j*) P. Fuentealba, H. Stoll, L. v. Szentpaly, P. Schwerdtfeger and H. Preuss, *J. Phys. B: At. Mol. Phys.*, 1983, **16**, L323–L328; (*k*) L. von Szentpály, P. Fuentealba, H. Preuss and H. Stoll, *Chem. Phys. Lett.*, 1982, **93**, 555–559; (*l*) P. Fuentealba, H. Preuss, H. Stoll and L. Von Szentpály, *Chem. Phys. Lett.*, 1982, **89**, 418–422; (*m*) T. H. Dunning and P. J. Hay, in *Modern theoretical chemistry*, Plenum Press, New York, 1977, vol. 3, p. 1; (*n*) A. Ehlers, M. Böhme, S. Dapprich, A. Gobbi, A. Höllwarth, V. Jonas, K. Köhler, R. Stegmann, A. Veldkamp and G. Frenking, *Chem. Phys. Lett.*, 1993, **208**, 111–114.

22 W. J. Hehre, R. Ditchfield and J. A. Pople, *J. Chem. Phys.*, 1972, **56**, 2257–2261.

23 R. Krishnan, J. S. Binkley, R. Seeger and J. A. Pople, *J. Chem. Phys.*, 1980, **72**, 650–654.

24 A. Bergner, M. Dolg, W. Küchle, H. Stoll and H. Preuß, *Mol. Phys.*, 1993, **80**, 1431–1441.

25 Solvent corrections were not included for these calculations since catalytic reactions were performed neat thus an appropriate solvent could not be chosen.

26 (*a*) S. Gorelsky, *AOMix Program for Molecular Orbital Analysis-Version 6.5*, University of Ottawa, Ottawa, Canada, 2011. URL: http://www.sg-chem.net; (*b*) S. Gorelsky and A. Lever, Electronic Structure and Spectra of Ruthenium Diimine Complexes by Density Functional Theory and INDO/S. Comparison of the Two Methods, *J. Organomet. Chem.*, 2001, **635**, 187–196.